ELSEVIER

Journal of Nuclear Materials 290–293 (2001) 678–682

journal of nuclear materials

www.elsevier.nl/locate/jnucmat

Island divertor in a helical-axis heliotron device (Heliotron J)

T. Mizuuchi [a,*], M. Nakasuga [b], F. Sano [a], Y. Nakamura [b], K. Nagasaki [a], H. Okada [a], K. Kondo [b], T. Obiki [a]

[a] *Institute of Advanced Energy, Kyoto University, Gokasho, Uji, Japan*
[b] *Graduate School of Energy Science, Kyoto University, Gokasho, Uji, Japan*

Abstract

A new configuration with $\iota/2\pi \sim 0.5$ is proposed as an island divertor configuration in Heliotron J, a small size $l = 1/M = 4$ helical-axis heliotron device. In this case, both the $m = 8/n = 4$ edge islands and the last closed flux surface can keep simultaneously the moderate size. As a first step of an island divertor design with this configuration, edge field characteristics are numerically investigated assuming a target plate at $r_{\text{target}} = 0.33$ m (5 cm inside from the chamber wall). It is shown that the divertor fields cross the target at four discrete regions per a field period. The connection length from the edge to the target plate is in the range of 50–400 m. The total value of the 'wetted area' for the whole torus is about 600 cm^2. The incidence angle of the diverted field lines to the target plate is less than 10°.

Keywords: Heliotron J; Divertor; Edge field topology

1. Introduction

To settle the particle control and heat handling issues for long pulse operation of fusion plasmas, a divertor is necessary in any magnetic confinement system. In heliotrons/stellarators, two types of divertor configuration are proposed, a helical and an island divertor (including an local island divertor (LID)). The former is usually observed in a high shear heliotron device such as Heliotron E [1] and LHD [2], where no external field is necessary to obtain the diverting field. In low shear stellarators, 'natural-islands' near the LCFS can be used as a divertor without any external perturbation fields. An island divertor design in W7-AS and W7-X is based on this idea [3]. It is also possible to make an island divertor in high shear devices by imposing external perturbation fields such as the LID in CHS and LHD [4].

All these configurations have a 3-D magnetic topology. The toroidal and poloidal inhomogeneity of divertor plasmas should be taken into account to understand experimental data [5]. Although some experiments have investigated divertor plasma properties for each configuration, the database is not enough to make detailed simulation models for such a 3-D configuration and to discuss each divertor scenario. More detailed investigations, especially comparative studies between a helical and an island divertor, are necessary to understand the characteristics of each divertor.

In Heliotron J, a helical-axis heliotron device newly constructed at the Institute of Advanced Energy, Kyoto University [6,7], the edge field topology can be varied from a helical-divertor to an island-divertor type divertor [8]. This is favorable to study the effect of edge structure on SOL/divertor plasmas and to examine the different divertor configurations. In [8], we reported two candidates for an island divertor configuration in Heliotron J. These configurations are, however, difficult to simultaneously keep enough size of the LCFS and the island size. In this paper, we propose a new configuration for a more preferable configuration to an island divertor in Heliotron J.

* Corresponding author. Tel.: +81-774 38 3451; fax: +81-774 38 3535.

E-mail address: t-mizuuchi@iae.kyoto-u.ac.jp (T. Mizuuchi).

0022-3115/01/$ - see front matter
PII: S0022-3115(00)00596-1

2. The Heliotron J device

In this section, the characteristics of the Heliotron J device and its field structure are briefly summarized [6–8]. Fig. 1 shows the top view of plasma with the helical field coil, HFC (an $l = 1/M = 4$ continuous coil) and the toroidal field coils. (Three pairs of poloidal field coils are not drawn.) The major radius of the HFC is $R_0 = 1.2$ m and the maximum field strength on the magnetic axis is $B = 1.5$ T. The average plasma minor radius is $\langle a_p \rangle \approx 0.1$–$0.2$ m. The obtainable range of the rotational transform is 0.3–0.8 with low shear. In contrast to the conventional planar-axis heliotron, one can produce the magnetic well in the whole confinement region to suppress the pressure driven instability at high β current-less plasmas. The bumpiness is a key component of the confinement field for improving the high-energy particle confinement, as well as for reducing the neoclassical transport [9].

The edge field topology is sensitive to the change of edge rotational transform. When $\iota/2\pi$ is far from any low mode resonance condition, no clear remaining island is observed outside the LCFS (Case-A [8]). This is a similar topology to that in a conventional heliotron. When $\iota/2\pi$ is close to a low rational number, a clear island chain is observed outside the LCFS without any perturbation field. The interesting modes of the natural island are $m/n = 8/4$ and $7/4$ in Heliotron J. Here, m and n are the poloidal and the toroidal mode numbers, respectively. In Case-B configuration in [8], the size of $m/n = 7/4$ islands in a poloidal cross-section is large enough and the center of these islands is positioned far from the LCFS. However, the average radius of the core plasma is only $\langle a_p \rangle \sim 0.1$ m. In Case-C in [8], the core plasma size is tolerable, $\langle a_p \rangle \sim 0.15$ m. However, the size of $m/n = 8/4$ islands is small and the center of the island is closed to the LCFS.

Further survey of the possible configuration brings us another $m/n = 8/4$ island configuration (Case-D) which has moderate size of the LCFS and the edge islands.

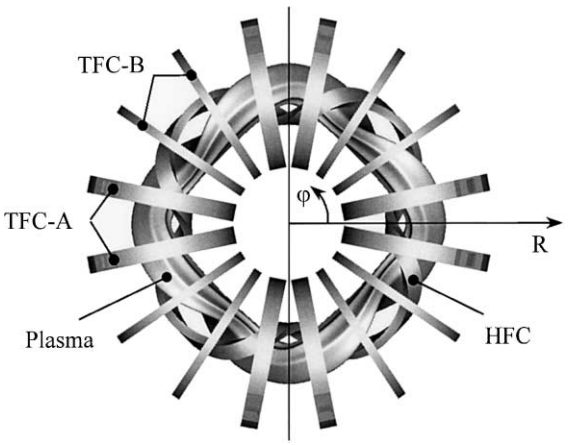

Fig. 1. A top view of plasma with the HFC and TFCs. The PFCs are not drawn. The origin of the toroidal angle φ in this paper is denoted.

3. The new $m/n = 8/4$ island configuration

Fig. 2 shows the calculated edge topology for the new $m/n = 8/4$ island configuration at different poloidal cross-sections. The value of $\iota/2\pi$ and the well depth at the plasma edge are ~0.495 and ~1%, respectively. The LCFS with $\langle a_p \rangle \sim 0.15$ m is surrounded by a chain of $m/n = 8/4$ islands with the radial size of ~0.1 m at $\varphi = 45°$. There is no closed magnetic surface outside the islands.

Although this topology seems preferable as an island divertor configuration, some parts of the island are positioned very closed to the vacuum chamber at the HFC side (Fig. 2(a) and (b)), where r_{wall} is small due to the HFC guide groove. To avoid the plasma contact at this side, target plates should be installed at the other proper positions so that the divertor plasma flow can be terminated before it reaches the wall at the HFC side. As a preliminarily consideration, let us consider a simple shape of the targets, a simple torus with $R = R_0$ and r_{target} only at the circular part of the wall ($r_{wall} = 0.38$ m). Here, we select $r_{target} = 0.33$ m to keep a sufficient clearance (about 2–3 cm) on the HFC side.

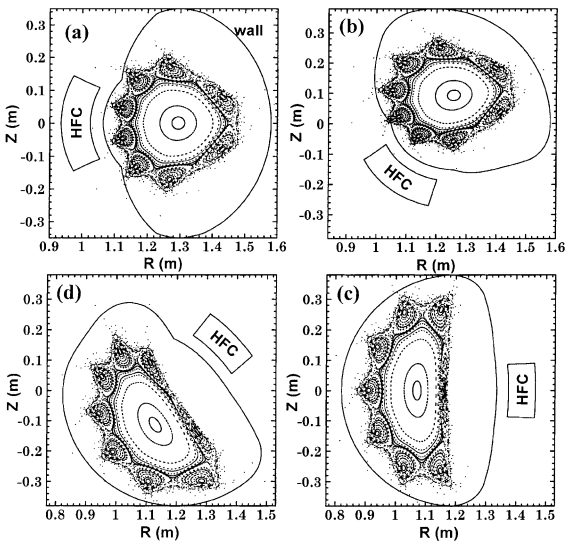

Fig. 2. The calculated field topology of the new island divertor configuration for different poloidal cross-sections: (a) the toroidal angle $\varphi = 0°$; (b) $\varphi = 10.5°$; (c) $\varphi = 45°$; (d) $\varphi = 61.5°$. Note that the toroidal angle for one field period is 90°.

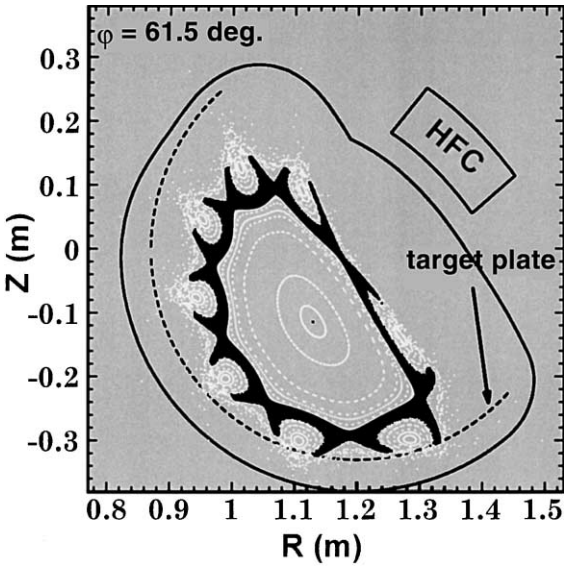

Fig. 3. Puncture plot of the divertor field lines with $r_{target} = 0.33$ m at $\varphi = 61.5°$. The two directional field traces are stopped when the field line cross the target plate. White lines show the field topology without the target plate and the vacuum chamber.

A Poincaré plot of the divertor field lines in this case is shown in Fig. 3. The field lines are starting from a zone of $\delta r \leqslant 1$ cm, $0° \leqslant \theta \leqslant 360°$ and $0° \leqslant \varphi \leqslant 45°$ (a half period) and traced up to the target plate, where δr is a radial distance from the LCFS.

3.1. Footprints of divertor field lines on the target plate

Fig. 4(a) shows the footprints of the field lines on the target plate in the toroidal–poloidal coordinate, (φ, θ). The starting points are selected randomly from the same zone described above. The divertor fields cross the target at four discrete regions per field period (A-1, A-2, B-1 and B-2 in Fig. 4(a)). The positions of A-1(2) and B-1(2) are symmetric each other. The direction of the field trace (CW or CCW in the toroidal direction) decides which field-lines reach the areas A or B. Only A(B)-1 or A(B)-2 are marked by one directional field trace.

From a 2-D histogram of the footprints, we can estimate a relative distribution of the hitting field lines on each area. One example for the area-A is shown in Fig. 4(b), where the coordinate system is ($L_{toroidal} = R \times \varphi$ (rad.), $L_{poloidal} = r_{target} \times \theta$ (rad.)). As shown in this figure, the field-line density is not uniform. The density in A-1 is much higher than A-2. In this sense, we can say that A-1 is the 'main' divertor target region.

From Fig. 4, we can roughly estimate a value of the 'wetted area' of the target plate. The total value for the whole torus is about 600 cm^2. This corresponds to about

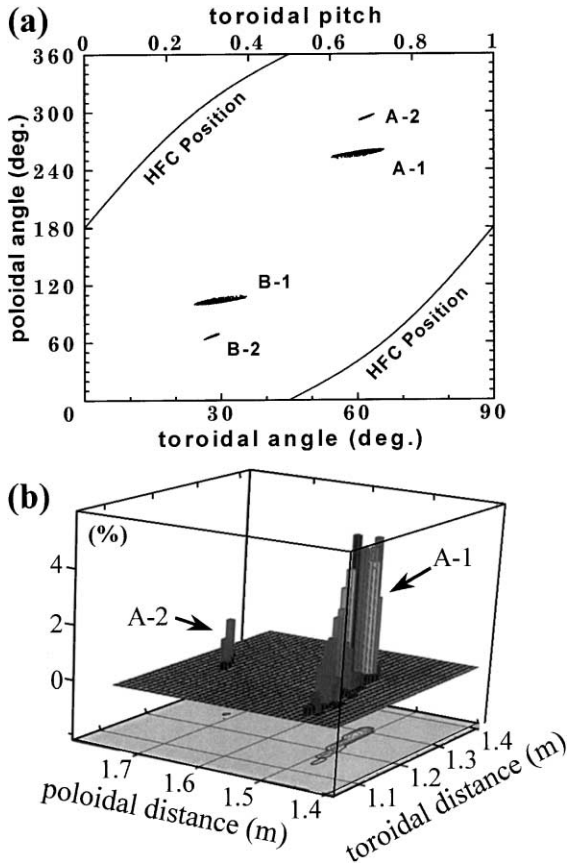

Fig. 4. (a) The footprint positions of the divertor field lines on the target plate in the (φ, θ) coordinate. The two solid curves show the HFC position; (b) a 2-D histogram of the footprints (Area-A in (a)).

1% of the total surface area of the LCFS. To make a fine estimation, we need to know the width of the SOL, which must be obtained from experiments in Heliotron J. In the Heliotron E case, a characteristic decay length of the density in the thick ergodic scrape-off region with long connection length is ~3–4 cm [10], which suggests that the SOL width for the heat flow would be 1–2 cm. The Heliotron J edge configuration discussed here is not an ergodic one. Therefore, the SOL width would be thinner than the value in Heliotron E if the perpendicular diffusion coefficients of the SOL plasma are almost the same as that in the Heliotron E SOL.

3.2. Connection length to the target plate

Fig. 5(a) shows a histogram of the connection lengths, L_c (the length of the field line from the start point to the target). The starting point is the same as in the case of Fig. 4. The range of L_c is 50–400 m and the average L_c (an arithmetic mean of the data in Fig. 5(a))

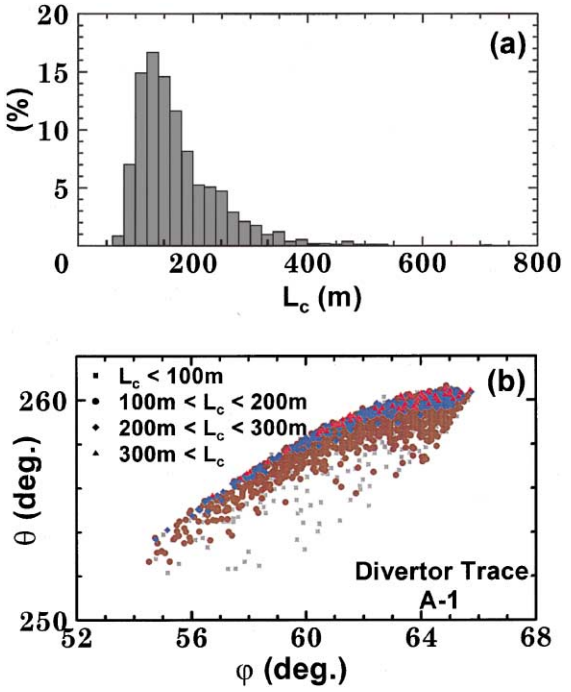

Fig. 5. (a) A histogram of the connection length of the field lines from the start point to the target plate (omitting the field lines that have a connection length longer than 1000 m); (b) the 'L_c-map' on the footprint area for A-1 in Fig. 4.

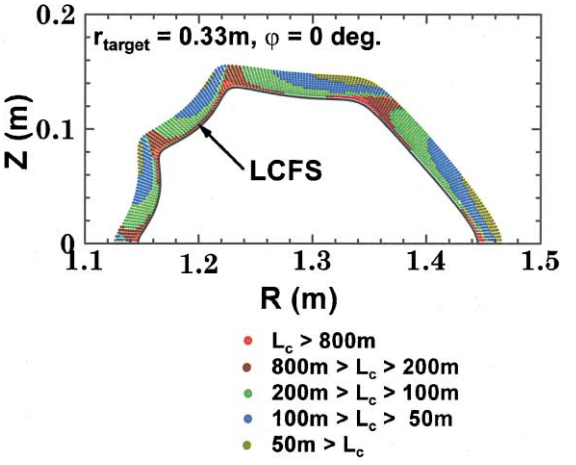

Fig. 6. A dependence of L_c on the starting point. The field trace starts from the point outside the LCFS at the $\varphi = 0°$.

is ≈150 m. Since the field line is traveling along the island, L_c becomes much longer than that in the tokamak-like case without islands where $L_c \sim q\pi R_0 \sim 8$ m for $q = 1/(\iota/2\pi) \sim 1/0.5$. This might be an advantage for obtaining a large temperature gradient between the SOL and the target plates. However, we must experimentally check the SOL width does not exceed the island width to use this configuration as the island divertor.

An 'L_c-map' of the A-1 footprint area is shown in Fig. 5(b). Although no clear structure is observed, field lines with longer L_c seem to come to the island separatrix side. On the other hand, the dependence of L_c on the starting point has a clear structure. Fig. 6 shows one example at $\varphi = 0°$, where the starting points (up to 2 cm outside the LCFS) are classified into five groups depending on L_c obtained from the one-way (CCW) calculation. The field lines starting near the X-point have longer L_c and those from the O-point have shorter L_c.

3.3. Direction of the divertor field lines

The incidence angle of the field lines into the target, α, where $\alpha = 0°$ means the field line is tangent to the target, is another important parameter from the viewpoint of the heat load to the divertor target. A small incidence angle can increase the effective wetted area of the divertor plate but requires the fine adjustment in the divertor tile setting to avoid the leading edge problem. Fig. 7(a) is the φ-dependence of α and (b) shows the corresponding histogram. The incidence angle of the field lines is less than 10°. The incidence angle is a

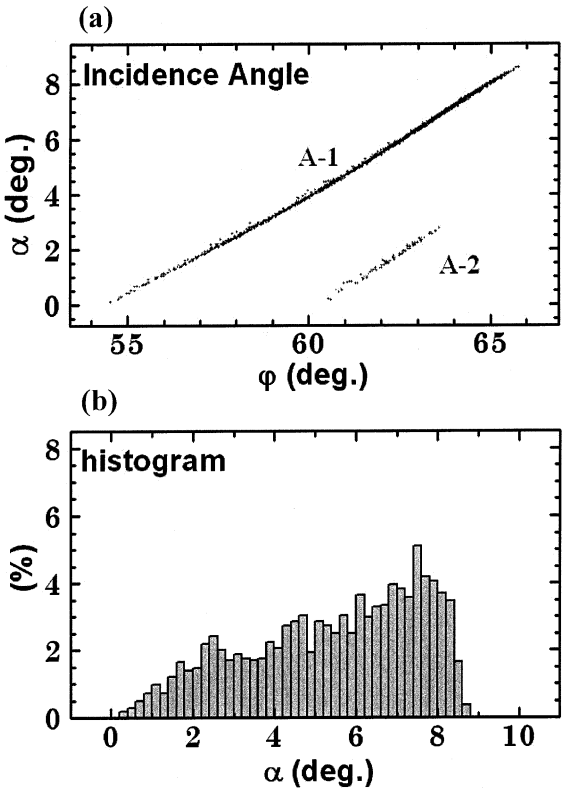

Fig. 7. (a) A toroidal angle dependence of the incidence angle; (b) a histogram of the incidence angle to the target plate.

function of φ and it is possible to reduce α by increasing r_{target}. When we set the target at $r_{\text{target}} = 0.35$ m, for e.g., the incidence angle becomes less than 6°. However, in this case, the clearance at the HFC side becomes severe and the wetted area is reduced.

The ratio of B_θ–B_φ is slightly different between A(B)-1 and A(B)-2 group; $B_\theta/B_\varphi \sim 0.26$–$0.3$ for A(B)-1 group and ~ 0.40–0.41 for A(B)-2 group. Since A(B)-2 group is closer to the helical coil, the poloidal field component becomes higher.

4. Summary and acknowledgements

A new configuration with $\iota/2\pi \sim 0.5$ is proposed for an island divertor configuration in Heliotron J. In contrast to the previous configurations, the proposed one can keep moderate size of $m = 8/n = 4$ islands and the size of the LCFS simultaneously.

As a first step of an island divertor design with this configuration, edge field characteristics are numerically investigated assuming a simple torus-shaped target plate at $r_{\text{target}} = 0.33$ m. It is shown that the divertor fields cross the target plate at four discrete regions ((main+sub.) $\times$ 2) per field period. The total value of the wetted area for the whole torus is about 600 cm^2. The connection length is in the range of 50–400 m and the averaged value is about 150 m. The incidence angle of the diverted field lines to the target plate is less than 10°. The ratio of B_θ–B_φ is $B_\theta/B_\varphi \sim 0.26$–$0.41$.

One disadvantage to an island divertor is its small wetted area. In the present case of Heliotron J, since the total heating power of $\sim$1 MW is expected in NBI experiments, an averaged heat load on the target will be about 10 MW/m^2 even the case of $P_{\text{rad}} \sim 40\%$. Taking the 'density profile' of the footprints into account, a peak heat load will be more increased. Although this may not be so a severe problem in Heliotron J due to the short pulse discharge, it is necessary to investigate for future devices how we can reduce the heat load density by optimizing the design of the target plate.

The values discussed in this paper, such as the wetted area, connection length and incidence angle, depend on the target plate design. Since we consider the simple torus-shape as the target plates in this paper, we can consider the obtained values as the basic characteristics of this field configuration. The modification of the target design can change not only the incidence angle and the connection length but also increase the number of the area where the divertor field reaches. Optimization of the shape and position of target plates will be performed by taking into account the experimental data on SOL/divertor plasma in addition to the more detailed field analyses.

The authors are grateful to the members of the Heliotron J Group for useful discussions and help. This work was partly supported by the Collaboration Program of the Laboratory for Complex Energy Process, IAE, Kyoto University.

References

[1] T. Mizuuchi et al., J. Nucl. Mater. 162–164 (1989) 105.
[2] N. Ohyabu et al., in: Plasma Physics Controlled Nuclear Fusion Research 1992, vol. 2, IAEA, Vienna, 1993.
[3] F. Sardei et al., J. Nucl. Mater. 241–243 (1997) 135.
[4] N. Ohyabu et al., J. Nucl. Mater. 220–222 (1995) 298.
[5] T. Mizuuchi et al., J. Nucl. Mater. 266–269 (1999) 1139.
[6] T. Obiki et al., in: 12th International Stellarator Conference, Wisconsin, USA, 1999.
[7] F. Sano et al., in: 10th International Toki Conference on Plasma Physics Nuclear Fusion, Toki, Japan, 2000, PII-9; J. Plasma Fus. Res. Ser., to be published.
[8] T. Mizuuchi et al., in: 10th International Toki Conference on Plasma Physics Nuclear Fusion, Toki, Japan, 2000, PI-19; J. Plasma Fusion Research Series, to be published.
[9] M. Wakatani et al., Nucl. Fus. 40 (3Y) (2000) 435.
[10] T. Mizuuchi et al., J. Nucl. Mater. 167–177 (1990) 1070.